Permeation of Hexane Isomers across ZSM-5 Zeolite Membranes

Rajamani Krishna* and Dietmar Paschek

Department of Chemical Engineering, University of Amsterdam, Nieuwe Achtergracht 166, 1018 WV Amsterdam, The Netherlands

Gump et al. (*Ind. Eng. Chem. Res.* **1999**, *38*, 2775) recently showed that extremely high selectivities are realized for the separation of normal hexane (n-C_6) from 2,2-dimethylbutane (22DMB) when these components are allowed to diffuse across a ZSM-5 zeolite membrane. Their reported selectivities for a 50−50 feed mixture was found to be about 2 orders of magnitude higher than that for the single components. Furthermore, at a temperature of 398 K, the flux of 22DMB exhibits a curious maximum with increasing partial pressure. The objective of this communication is to provide a theoretical background to their experimental observations. Configurational bias Monte Carlo (CBMC) simulations are used to calculate the pure component and mixture isotherms at various temperatures. The Maxwell−Stefan (MS) theory for zeolite diffusion is then used to calculate the fluxes for single-component and binary-mixture permeation. The combined CBMC−MS model provides a nearly quantitative explanation of the experimental data of Gump et al.

1. Introduction

In a recent paper Gump et al.[1] reported permeation data for normal hexane (n-C_6) and 2,2-dimethylbutane (22DMB) through two ZSM-5 zeolite membranes, named M1 and M2. For membrane M2, the permeation rates were studied as a function of temperature (T = 353, 373, and 398 K) for a 50−50 mixture of n-C_6 and 22DMB. For membrane M1, the temperature was maintained at T = 373 K and the permeation rates were studied for a range of organics content of the feed vapor mixture in a helium carrier gas and variation of the n-C_6 mole fraction in the organic feed (y_1 = 0.1, 0.2, 0.3, 0.4, 0.5, 0.6, and 0.8). Several interesting and nonintuitive results have been reported:

(a) The selectivity for the separation of n-C_6 from 22DMB for experiments with M2 is about a couple of orders of magnitude higher than that which would have been expected for the pure component permeation data.

(b) For experiments at 398 K with membrane M2, the flux of 22DMB exhibits a curious maximum with increasing partial pressure.

(c) For experiments with membrane M1, the flux of 22DMB again exhibits a curious maximum with varying organics content in the feed mixture.

The objective of this communication is to provide a fundamental background to the permeation experiments of Gump et al. and to develop a model that provides a near-quantitative description of the measured fluxes of n-C_6 and 22DMB. We start by using configurational bias Monte Carlo simulations to generate the necessary pure component and mixture isotherms at various temperatures. The Maxwell−Stefan theory of zeolite diffusion is then used to predict the mixture fluxes on the basis of information on single-component permeation characteristics.

2. Configurational Bias Monte Carlo Simulations

Our earlier studies have demonstrated the power of CBMC simulations in the grand canonical ensemble for calculation of sorption isotherms;[2−4] we shall use the same simulation technique here to calculate the isotherms of the pure components n-C_6 and 22DMB and of the mixture in ZSM-5, taken to be equivalent to silicalite-1 with regard to the sorption characteristics. Our simulations have been performed in the grand canonical ensemble wherein the zeolite is in contact with a reservoir that fixes the chemical potential of each component and also the temperature. In a CBMC simulation, it is essential to successfully exchange particles with the reservoir. With this technique we grow a flexible alkane molecule atom by atom in such a way that the "empty spaces" in the zeolite are found. The bias of this growing scheme is removed exactly by a modification of the acceptance rules.[4] The acceptance ratio of the particle exchange move is increased by 10 to 100 orders of magnitude and thus makes these simulations possible. To increase the efficiency for the mixture simulations, we also performed trial moves which change the identity of a particle.[4] In the simulations presented in this work the linear and branched alkanes are described with a united-atom model; i.e., CH_3, CH_2, and CH groups are considered as single-interaction centers. The zeolite is assumed to be rigid and the interactions of the alkane with the zeolite are dominated by the oxygen atoms of the zeolite. The alkane−zeolite and alkane−alkane interactions are described by a Lennard-Jones potential. The intramolecular interactions include bond bending and torsion potentials and a fixed C−C bond length. The force-field parameters are reported in ref 4.

Our simulation box consists of 16 ($2 \times 2 \times 4$) unit cells of silicalite. The simulations are performed in cycles; in each cycle an attempt is made to perform one of the following moves: (1) displacement of a chain (a chain is selected at random and given a random displacement), (2) rotation of a chain (a chain is selected at random and given a random rotation around the center of mass), (3) partial regrowing of a chain (a chain is selected at random and part of the molecule is regrown using the CBMC scheme), (4) exchange with the reservoir using the CBMC scheme (it is decided at random whether to add or to remove a molecule from the zeolite), and (5) change of identity (only in the case of mixtures) (one of the components is selected at

* To whom correspondence should be addressed. Fax: +31 20 5255604. E-mail: krishna@its.chem.uva.nl.

10.1021/ie990912d CCC: $19.00
Published on Web 05/26/2000

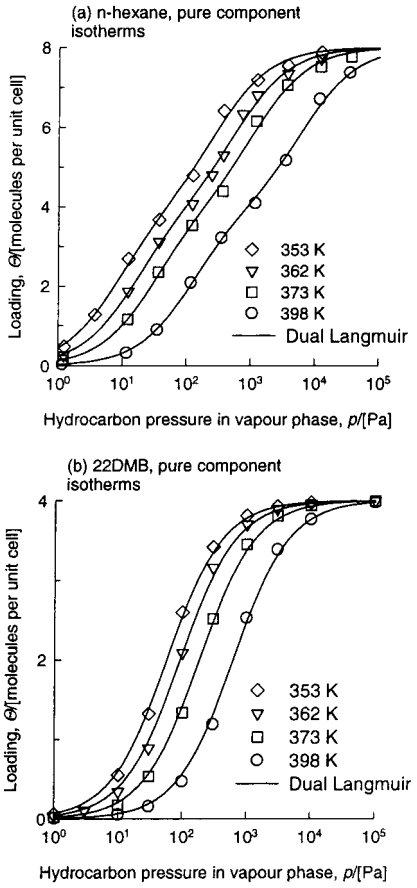

Figure 1. Pure component isotherms for (a) *n*-C_6 and (b) 22DMB at various temperatures in silicalite-1. The symbols represent the CBMC simulations. The continuous lines are the dual-site Langmuir (DSL) model (eq 1) with parameters given by eqs 2 and 3.

random and an attempt is made to change its identity). The acceptance rules for this type of move are given elsewhere.[4] A total simulation consisted of at least 300 000 Monte Carlo cycles.

The CBMC simulations for pure components *n*-C_6 and 22DMB were carried out at four different temperatures (353, 362, 373, and 398 K). These simulation results are shown in Figure 1. The sorption isotherms could be fitted accurately with a dual-site Langmuir model:

$$\Theta_1 = \frac{\Theta_{\text{sat,A}} b_{1,\text{A}} p_1}{1 + b_{1,\text{A}} p_1} + \frac{\theta_{\text{sat,B}} b_{1,\text{B}} p_1}{1 + b_{1,\text{B}} p_1} = [(\Theta_{\text{sat,A}} b_{1,\text{A}} + \Theta_{\text{sat,B}} b_{1,\text{B}}) p_1 + (\Theta_{\text{sat,A}} + \Theta_{\text{sat,B}}) b_{1,\text{A}} b_{1,\text{B}} p_1^2]/[1 + (b_{1,\text{A}} + b_{1,\text{B}}) p_1 + b_{1,\text{A}} b_{1,\text{B}} p_1^2] \quad (1)$$

In setting up eq 1 we identify two distinct adsorption sites: (1) site A, which represents the intersections between the straight channels and the zigzag channels, and (2) site B, which represents the channel interiors. Normal hexane (component 1) shows a slight inflection at a loading of four molecules per unit cell and so we take $\Theta_{\text{sat,A}} = 4$. The total loading $\Theta_{\text{sat,A}} + \Theta_{\text{sat,B}} = \Theta_{\text{sat}} = 8$. The isotherms for normal hexane could be fitted with the following temperature dependence

$$b_{1,\text{A}} = 6.82 \times 10^{-12} \exp\left(\frac{69\,140}{RT}\right); \quad b_{1,\text{B}} = 5.087 \times 10^{-15} \exp\left(\frac{80\,000}{RT}\right) \quad (2)$$

The 22DMB (component 2) prefers to occupy the intersections (site A) and even increasing pressures to 10^7 Pa is insufficient to drive these molecules into the channel interiors. The Langmuir constants for this species are described by

$$b_{2,\text{A}} = 1.025 \times 10^{-11} \exp\left(\frac{62\,430}{RT}\right); \quad b_{2,\text{B}} = 0 \quad (3)$$

The CBMC simulations for a 50−50 mixture at temperatures of T = 362, 373, and 398 K are shown in Figure 2. It is remarkable to note that the 22DMB loading exhibits a maximum with increasing partial pressure. As the partial pressures increase to 100 Pa, the sorbate loading of both linear and branched alkanes increases until a maximum is reached in the loading of 22DMB. This occurs at a total loading of four molecules per unit cell. Up to this point there is really no competition between *n*-C_6 and 22DMB and both are almost equally easily adsorbed. A snapshot of the CBMC simulation at 100 Pa and 373 K is given in Figure 3. This shows that all the 22DMB molecules are located at the intersections between the straight channels and the zigzag channels whereas *n*-C_6 molecules are located everywhere. The *n*-C_6 molecules fit nicely into both straight and zigzag channels; these molecules have a higher "packing efficiency" than 22DMB. As the pressure is increased beyond 100 Pa, it is more efficient to obtain higher loading by "replacement" of the 22DMB with *n*-C_6; this *configurational entropy* effect is the reason behind the curious maximum in the 22DMB isotherm. For partial pressures higher than about 10^4 Pa the 22DMB is virtually excluded from the zeolite.

The curious mixture isotherm is reasonably well represented by the mixture rule

$$\Theta_i = [(\Theta_{\text{sat,A}} b_{i,\text{A}} + \Theta_{\text{sat,B}} b_{i,\text{B}}) p_i + (\Theta_{\text{sat,A}} + \Theta_{\text{sat,B}}) b_{i,\text{A}} b_{i,\text{B}} p_i^2]/[1 + (b_{1,\text{A}} + b_{1,\text{B}}) p_1 + b_{1,\text{A}} b_{1,\text{B}} p_1^2 + (b_{2,\text{A}} + b_{2,\text{B}}) p_2 + b_{2,\text{A}} b_{2,\text{B}} p_2^2] \quad i = 1, 2 \quad (4)$$

The continuous lines in Figure 2 have been drawn using eqs 2−4.

3. The Maxwell−Stefan Diffusion Model for Membrane Permeation

The Maxwell−Stefan theory of zeolite diffusion[5−9] is used to relate the molar fluxes N_i to the chemical potential gradients by

$$-\frac{\Theta_i}{RT}\frac{\rho}{A}\nabla_{\text{T}}\mu_i = \sum_{\substack{j=1 \\ j\neq i}}^{n} \frac{\Theta_j N_i - \Theta_i N_j}{\Theta_{\text{sat}} Đ_{ij}} + \frac{N_i}{Đ_i}, \quad i = 1,2,\ldots n \quad (5)$$

In eq 5 A represents the Avogadro number = 6.023×10^{23} molecules/mol and ρ is the zeolite density expressed in the number of unit cells per cubic millimeter of zeolite. We have to reckon in general with two types of Maxwell−Stefan diffusivities: $Đ_{ij}$ and $Đ_i$. The $Đ_i$ can essentially be identified with Maxwell−Stefan diffusivity for single-component diffusion. Mixture diffusion introduces an additional complication due to sorbate−sorbate interactions. This interaction is embodied in the coefficients $Đ_{ij}$. We can consider this coefficient as representing the facility for counterexchange; that is, at a sorption site the sorbed species j is replaced by the species i. The net effect of this counterexchange is a

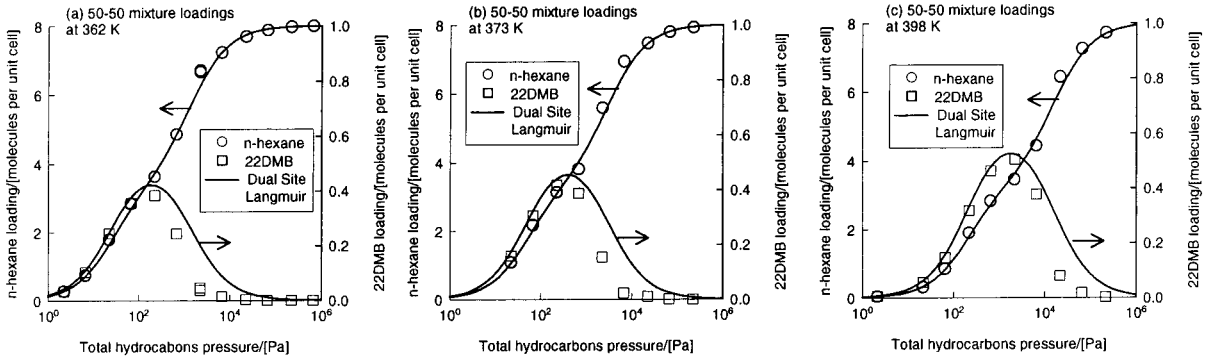

Figure 2. CBMC simulations of the 50−50 mixture isotherm at (a) 362, (b) 373, and (c) 398 K.

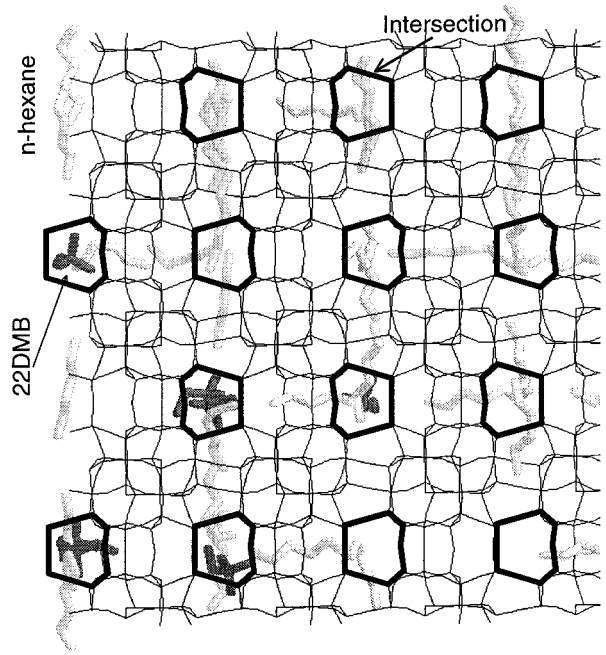

Figure 3. Snapshot of CBMC simulation of the 50−50 mixture at 373 K and 100 Pa.

slowing down of a faster moving species due to interactions with a species of lower mobility. Also, a species of lower mobility is accelerated by interactions with another species of higher mobility. The effect of the interchange diffusivity becomes important when the species have widely different mobilities.[10] For modeling the *n*-C_6−22DMB mixture permeation we ignore these interactions because the ratio of $Đ_1/Đ_2$ is found to be only 3.5 from the single-component permeation data,[1] as will be seen later. With this simplification the molar fluxes can be rewritten in compact two-dimensional matrix notation as

$$(\mathbf{N}) = -\frac{\rho}{A}\begin{bmatrix} Đ_1 & 0 \\ 0 & Đ_2 \end{bmatrix}[\mathbf{\Gamma}]\nabla(\mathbf{\Theta}) \tag{6}$$

The elements of the matrix of thermodynamic correction factors [**Γ**]

$$\Gamma_{ij} \equiv \frac{\Theta_i}{p_i}\frac{\partial p_i}{\partial \Theta_j}, \quad i, j = 1, 2 \tag{7}$$

can be determined by analytic differentiation of eq 4 and explicit algebraic expressions are available in Krishna et al.[8] For steady-state binary permeation across a

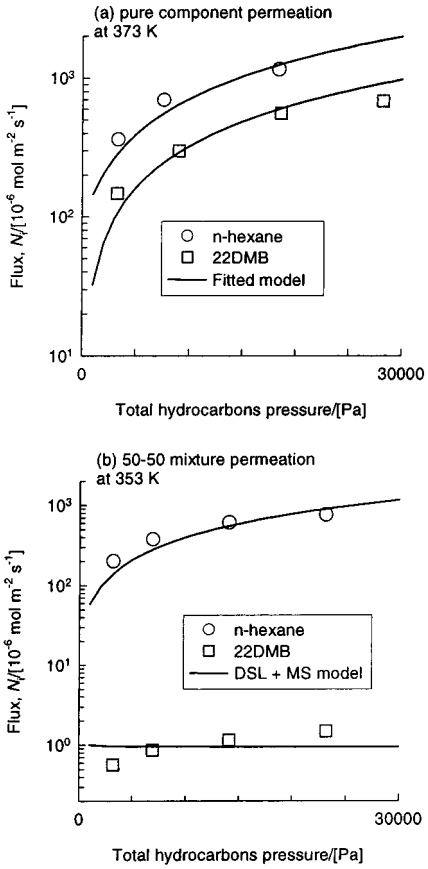

Figure 4. (a) Pure component permeation fluxes of *n*-C_6 and 22DMB at 373 K with membrane M2. Experimental data of Gump et al. (cf. their Figure 4) compared with model fits. (b) Binary 50−50 mixture permeation fluxes for *n*-C_6 and 22DMB at 353 K with membrane M2. Experimental data of Gump et al. (cf. their Figures 5 and 6) compared with model predictions.

zeolite membrane of thickness δ, the expression (6) can be integrated to obtain

$$(\mathbf{N}) = -\frac{\rho}{A\delta}\begin{bmatrix} Đ_1 & 0 \\ 0 & Đ_2 \end{bmatrix}[\mathbf{\Gamma}]\Delta(\mathbf{\Theta}) \tag{8}$$

For pure component permeation eq 8 simplifies to

$$N_i = -\frac{\rho}{A\delta} Đ_i \Gamma_i \Delta\Theta_i \tag{9}$$

where

$$\Gamma_i \equiv \frac{\Theta_i}{p_i}\frac{\partial p_i}{\partial \Theta_i} \tag{10}$$

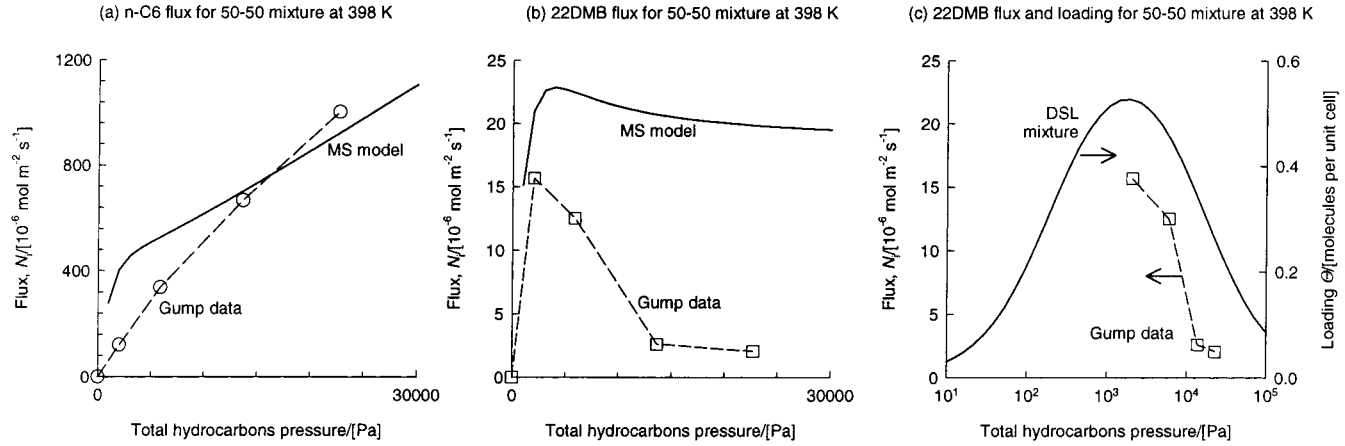

Figure 5. Binary 50−50 mixture permeation fluxes for (a) *n*-C_6 and (b) 22DMB at 398 K with membrane M2. Experimental data of Gump et al. (cf. their Figures 5 and 6) compared with Maxwell−Stefan model predictions.

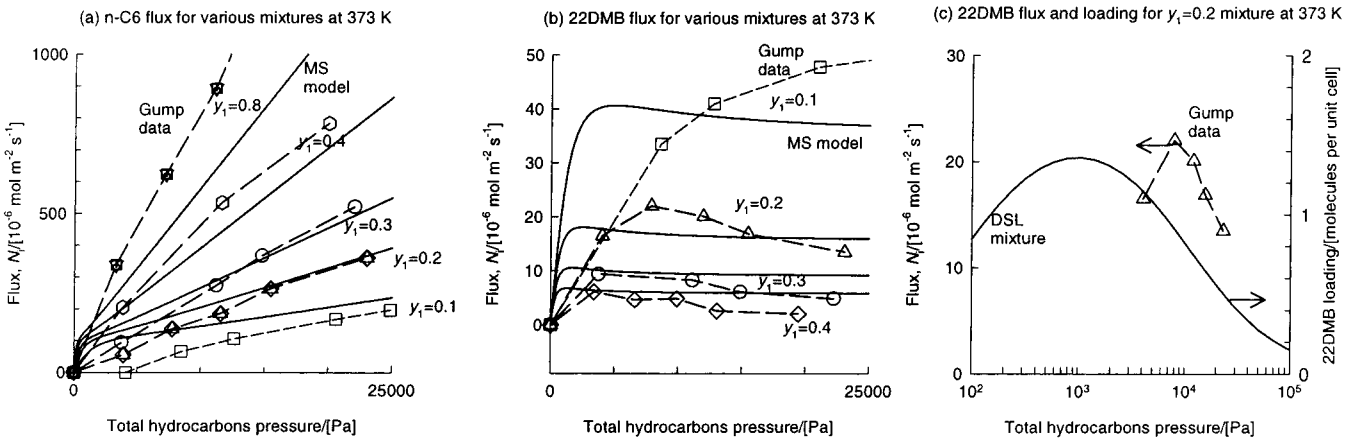

Figure 6. Binary mixture permeation fluxes for (a) *n*-C_6 and (b) 22DMB at 373 K with membrane M1. Experimental data of Gump et al. (cf. their Figures 1 and 2) compared with Maxwell−Stefan model predictions. To interpret the experimental data, the upstream partial pressure was taken to be 84 kPa.

can be determined by analytic differentiation of the pure component isotherms (1); an explicit algebraic expression has been derived by Krishna et al.[8]

4. Simulation of Permeation Experiments of Gump et al.

First, we consider the single-component fluxes determined in membrane M2 by Gump et al.[1] at a temperature of 373 K (cf. Figure 4 of this paper). The fitted single-component isotherms (eqs 2 and 3) and the measured data were used to determine the value of $(\rho/A\delta)Đ_1$ for *n*-C_6 to be 5×10^{-6}. The model predictions using this value for *n*-C_6 are shown in Figure 4a. The experimental data for 22DMB could be fitted when $Đ_1/Đ_2 = 3.5$ is taken (cf. Figure 4a). It is noteworthy that the ratio of diffusivities obtained from the permeation data of Gump et al. is significantly lower than the ratio obtained from the pure component diffusivities measured by Cavalcante and Ruthven.[11] For estimation of the diffusivities at temperatures other than 373 K we take an activation energy of 70 kJ/mol, for both components, on the basis of the information available in Cavalcante and Ruthven.[11] The model, tuned to take account of the membrane parameters and the temperature dependence of sorption and diffusion, is now ready to predict the mixture permeation results.

First, we consider the 50−50 mixture permeation experiments with membrane M2 at temperatures of 353 K. The model calculations at 353 K compare very well with the experimental data; see Figure 4b. In the model calculations we assume that the partial pressures of the permeating components at the downstream membrane compartment are vanishingly small. The high selectivities for mixture permeation are due to the virtual exclusion of the 22DMB at pressures exceeding 10^3 Pa (cf. Figure 2b).

For the 50−50 mixture permeation experiment at 398 K, the comparison between model calculations and experiments is shown in Figure 5a,b. The flux of *n*-C_6 is reasonably well predicted. The curious maximum in the flux of 22DMB is also reproduced in the simulations. The agreement of the model calculations and experiments for the 22DMB flux is less good because the assumption made in the model calculations that the downstream partial pressures are vanishingly small has a greater impact on the simulated values of 22DMB fluxes. Even so, the correct trend is reproduced. In Figure 5c the 22DMB flux and its loading (calculated using eq 4) have been plotted versus the hydrocarbons pressure. It is to be noted that the maximum in the 22DMB flux occurs at the same pressure at which the loading exhibits a maximum. For hydrocarbon pressures to the left of the maximum point in the loading, an increase of *P* will increase the 22DMB flux. To the right of the maximum, an increase in total *P* will result in a decrease in the 22DMB flux. The experiments of Gump et al.[1] were conducted on the right side of the peak.

For membrane M1, Gump et al.[1] report mixture permeation data for which the mixture composition has been varied from 10% to 80% of *n*-C_6 in the organic feed. These experimental results have been simulated. The curious maximum in the 22DMB flux, observed when the mole fraction organics in the feed is higher than 0.1, is reproduced qualitatively; see Figure 6a,b. The experimental flux of 22DMB at $y_1 = 0.2$ is highlighted for analysis in Figure 6c. The flux is compared with the loading of 22DMB, calculated from eq 4, taking $y_1 = 0.2$. The maximum in the flux occurs close to the pressure at which the loading of 22DMB in the mixture exhibits a maximum.

5. Conclusions

With the aid of CBMC simulations, it is shown that the extremely high selectivities reported by Gump et al.[1] for the separation of *n*-C_6 from 22DMB are primarily caused by the exclusion of 22DMB from the zeolite. The reason for this exclusion is to be found in configurational entropy effects. Our explanation is essentially different from that proposed by Gump et al., who consider the *n*-hexane to effectively block the permeation of 22DMB through nonzeolite pores.

The experimentally reported fluxes can be modeled nearly quantitatively by use of the Maxwell−Stefan theory for zeolite diffusion.

The curious maximum in the 22DMB flux observed in the experiments of Gump et al.[1] is explained by the fact that in the experiments the hydrocarbons total pressure corresponded to conditions near the maximum in the loading of 22DMB in the mixture isotherms. On one hand, an increase in the pressure for conditions to the *left* of the maximum leads to an *increase* in the 22DMB flux. On the other hand, an increase in the pressure to the *right* of the loading maximum leads to a *decrease* in the flux.

We have also shown that the experimental data of Gump et al. is amenable to interpretation in terms of intracrystalline sorption and diffusion.

We conclude the CBMC simulations, coupled with the Maxwell−Stefan diffusion equations, are a powerful tool for describing the separation performance of hydrocarbon mixtures in zeolite membranes.

Acknowledgment

R.K. and D.P. acknowledge a generous grant "Programmasubsidie" from The Netherlands Organisation for Scientific Research (NWO). The CBMC simulations were carried out using the BIGMAC program, authored by T. J. H. Vlugt, and is available on the web: http://molsim.chem.uva.nl/bigmac/. T. J. H. Vlugt is gratefully acknowledged for assistance with preparing the input data.

Notation

A = Avogadro number, 6.023×10^{23} molecules mol^{-1}
b_i = parameter in the dual-site Langmuir isotherm, Pa^{-1}
$Đ_i$ = Maxwell−Stefan diffusivity of species i in zeolite, m^2/s
$Đ_{ij}$ = Maxwell−Stefan diffusivity describing interchange between i and j, m^2/s
N_i = molar flux of species i, mol m^{-2} s^{-1}
P = total system pressure, Pa
p_i = partial pressure of species i, Pa
R = gas constant, 8.314 J mol^{-1} K^{-1}
T = absolute temperature, K
y_i = mole fraction of species i in the vapor mixture, dimensionless

Greek Letters

δ = thickness of membrane, m
Γ = thermodynamic correction factor, dimensionless
$[\Gamma]$ = matrix of thermodynamic factors, dimensionless
Θ_i = molecular loading, molecules per unit cell
$\Theta_{i,sat}$ = saturation loading, molecules per unit cell
$\Theta_{sat,A}$ = maximum loading of site A, molecules per unit cell
$\Theta_{sat,B}$ = maximum loading of site B, molecules per unit cell
Θ_{sat} = maximum loading in the zeolite, $\Theta_{sat} = (\Theta_{sat,A} + \Theta_{sat,B})$
μ_i = molar chemical potential, J mol^{-1}
ρ = density of membrane, number of unit cells per m^3

Subscripts

A = referring to site A, intersections
B = referring to site B, channel interiors
1 = component 1 in binary mixture
2 = component 2 in binary mixture
sat = referring to saturation conditions
i,j = components in mixture

Literature Cited

(1) Gump, C. J.; Noble, R. D.; Falconer, J. L. Separation of Hexane Isomers through Nonzeolite Pores in ZSM-5 Zeolite Membranes. *Ind. Eng. Chem. Res.* **1999**, *38*, 2775−2781.

(2) Vlugt, T. J. H.; Zhu, W.; Kapteijn, F.; Moulijn, J. A.; Smit B.; Krishna, R. Adsorption of Linear and Branched Alkanes in the Zeolite Silicalite-1. *J. Am. Chem. Soc.* **1998**, *120*, 5599−5600.

(3) Krishna, R.; Smit, B.; Vlugt, T. J. H. Sorption-Induced Diffusion-Selective Separation of Hydrocarbon Isomers Using Silicalite. *J. Phys. Chem. A* **1998**, *102*, 7727−7730.

(4) Vlugt, T. J. H.; Krishna, R.; Smit, B. Molecular Simulations of Adsorption Isotherms of Linear and Branched Alkanes and Their Mixtures in Silicalite. *J. Phys. Chem. B* **1999**, *103*, 1102−1118.

(5) Krishna, R. Multicomponent Surface Diffusion of Adsorbed Species. A Description Based on the Generalized Maxwell−Stefan Diffusion Equations. *Chem. Eng. Sci.* **1990**, *45*, 1779−1791.

(6) Krishna, R. Problems and Pitfalls in the Use of the Fick Formulation for Intraparticle Diffusion. *Chem. Eng. Sci.* **1993**, *48*, 845−861.

(7) Krishna, R.; Wesselingh, J. A. The Maxwell−Stefan Approach to Mass Transfer. C*hem. Eng. Sci* **1997**, *52*, 861−911.

(8) Krishna, R.; Vlugt, T. J. H.; Smit, B. Influence of Isotherm Inflection on Diffusion in Silicalite. *Chem. Eng. Sci.* **1999**, *54*, 1751−1757

(9) Kapteijn, F.; Moulijn, J. A.; Krishna, R. The Generalized Maxwell−Stefan Model for Diffusion in Zeolites: Sorbate Molecules with Different Saturation Loadings. *Chem. Eng. Sci.* **2000**, *55*, 2923−2930.

(10) Van de Graaf, J.; Kapteijn, F.; Moulijn, J. A. Modeling Permeation of Binary Mixtures through Zeolite Membranes. *AIChE J.* **1999**, *45*, 497−511.

(11) Cavalcante, C. L., Jr.; Ruthven, D. M. Adsorption of Branched and Cyclic Paraffins in Silicalite. 2. Kinetics. *Ind. Eng. Chem. Res.* **1995**, *35*, 185−191.

Received for review December 21, 1999
Revised manuscript received April 10, 2000
Accepted April 19, 2000

IE990912D